Fracture Phenomena in Advanced Fiber Composite Materials

H. J. KONISH JR.,* J. L. SWEDLOW,† AND T. A. CRUSE‡
Carnegie-Mellon University, Pittsburgh, Pa.

The extension of linear elastic fracture mechanics (LEFM) from metallic alloys to advanced fiber composite laminates is considered. LEFM is shown to be applicable to both isotropic and anisotropic homogeneous continua; the applicability of LEFM to advanced fiber composites is thus dependent on the validity of a homogeneous continuum model for such materials. An experimental program to determine the validity of such a model for graphite/epoxy laminates is reviewed. Such laminates are found to have an apparent fracture toughness, from which it is inferred that a homogeneous material model is appropriate for the particular specimen geometry and composite laminates considered. Strain energy release rates are calculated from the experimentally determined fracture toughnesses of the test laminates. These strain energy release rates fall into two distinct groups, corresponding to fracture across fibers and fracture between fibers. The latter case is further investigated. It is concluded that matrix fracture is governed by the tensile stress normal to the crack path.

Introduction

IT is a widely recognized fact that the presence of a crack or sharp flaw in a structural member dramatically reduces the load-carrying capacity of that member; consequently, a significant amount of technical effort has been directed toward the characterization and quantification of this phenomenon. The portion of this effort concerned with the analysis of static cracks in homogeneous, linear elastic continua has generated a body of theoretical and experimental information termed linear elastic fracture mechanics (LEFM). The applicability of LEFM to metallic alloys, which may be modelled as homogeneous isotropic continua, has been well established.

The present discussion is concerned with the applicability of LEFM to advanced fiber composite materials, which are neither homogeneous nor isotropic. Thus, the utilization of metals-based LEFM on advanced fiber composites is possible only if the heterogeneity and anisotropy of such materials are treated.

Analytical Model

Isotropic Materials

The analytical basis of LEFM is a series expression for the stress field induced in an unbounded, remotely loaded, two-dimensional structure by the presence of a line crack. For Mode I (in-plane, crack-symmetric) loading, the crack-induced stress field is[1]

$$\sigma_x = K_I(2\pi r)^{-1/2}\cos(\theta/2)[1-\sin(\theta/2)\sin(3\theta/2)]+0[(r/a)^0]$$
$$\sigma_y = K_I(2\pi r)^{-1/2}\cos(\theta/2)[1+\sin(\theta/2)\sin(3\theta/2)]+0[(r/a)^{1/2}]$$
$$\tau_{xy} = K_I(2\pi r)^{-1/2}\cos(\theta/2)\sin(\theta/2)\sin(3\theta/2)+0[(r/a)^{1/2}] \quad (1)$$

where (x,y) and (r,θ) are cartesian and polar coordinates, respectively (Fig. 1), a is the half-length of the crack, and K_I is the Mode I stress intensity factor, a function of loading conditions (hence the subscript I) and geometry. For Mode II (in-plane, crack-antisymmetric) loading, the crack-induced stress field is[1]

$$\sigma_x = -K_{II}(2\pi r)^{-1/2}\sin(\theta/2)[2+\cos(\theta/2)\cos(3\theta/2)]+0[(r/a)^{1/2}]$$
$$\sigma_y = K_{II}(2\pi r)^{-1/2}\sin(\theta/2)\cos(\theta/2)\cos(3\theta/2)+0[(r/a)^{1/2}]$$
$$\tau_{xy} = K_{II}(2\pi r)^{-1/2}\cos(\theta/2)[1-\sin(\theta/2)\sin(3\theta/2)]+0[(r/a)^{1/2}] \quad (2)$$

where K_{II} is the Mode II stress intensity factor.

Within a region in which r/a is small (the crack-tip region) the crack-induced stress fields (1, 2) are clearly dominated by the first terms of the series. The magnitudes of the stresses within this crack-tip region are therefore determined by the value of the appropriate stress intensity factor. Thus, if crack growth is posited to be a stress-governed phenomenon, the initial of crack growth in a given material may be characterized by some critical value of the appropriate stress intensity factor for a given structural geometry. Once this critical stress intensity factor (fracture toughness) has been determined for a given material, it is then possible to predict the critical load for other flawed structures of the same material, but of different geometries.

Anisotropic Materials

As just noted, the extension of LEFM procedures to advanced fiber composites must include a treatment of the heterogeneity and anisotropy of such materials. The anisotropy issue is dealt with easily, if the heterogeneity problem is temporarily avoided by assuming the homogeneous continuum model of a fiber composite obtained from lamination theory[2] to be a valid material representation. A stress analysis may then be performed on the

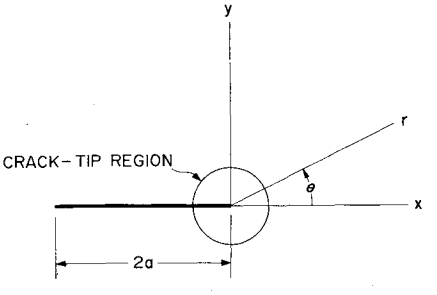

Fig. 1 Coordinate systems for the crack-tip region. The actual crack-tip region is a disk of "small" radius, centered at the crack tip.

Presented as Paper 72-384 at the AIAA/ASME/SAE 13th Structures, Structural Dynamics, and Materials Conference, San Antonio, Texas, April 10–12, 1972; submitted April 26, 1972; revision received July 31, 1972. The authors are pleased to acknowledge the joint support of this work by NASA, under NASA Research Grant NGR-39-002-023, and the United States Air Force, under Air Force Contract F33615-70-C-1146.

Index categories: Aircraft Structural Materials; Properties of Materials; Structural Composite Materials (Including Coatings).

* Graduate Student, Department of Mechanical Engineering.

† Associate Professor, Department of Mechanical Engineering. Associate Fellow AIAA.

‡ Associate Professor, Department of Mechanical Engineering. Member AIAA.

same unbounded two-dimensional structural model considered in the isotropic case, combined with this anisotropic material model, to yield series expressions for the crack-induced stress fields in an anisotropic material. For Mode I loading, the crack-induced stress field is[3,4]

$$\sigma_x = K_I(2\pi r)^{-1/2}Re\{[\mu_1\mu_2/(\mu_1-\mu_2)][\mu_2(\cos\theta+\mu_2\sin\theta)^{-1/2}-\mu_1(\cos\theta+\mu_1\sin\theta)^{-1/2}]\}+K_I(\pi a)^{-1/2}Re\{\mu_1\mu_2\}+0[(r/a)^{1/2}]$$

$$\sigma_y = K_I(2\pi r)^{-1/2}Re\{[1/(\mu_1-\mu_2)][\mu_1(\cos\theta+\mu_2\sin\theta)^{-1/2}-\mu_2(\cos\theta+\mu_1\sin\theta)^{-1/2}]\}+0[(r/a)^{1/2}] \quad (3)$$

$$\tau_{xy} = K_I(2\pi r)^{-1/2}Re\{[\mu_1\mu_2/(\mu_1-\mu_2)][(\cos\theta+\mu_1\sin\theta)^{-1/2}-(\cos\theta+\mu_2\sin\theta)^{-1/2}]\}+0[(r/a)^{1/2}]$$

where μ_1 and μ_2 are the distinct complex roots of

$$\beta_{11}\mu^4-2\beta_{16}\mu^3+(2\beta_{12}-\beta_{66})\mu^2-2\beta_{26}\mu+\beta_{22}=0 \quad (4)$$

with β_{ij} being the components of the compliance matrix of the laminate. For Mode II loading, the crack-induced stress field is[3,4]

$$\sigma_x = K_{II}(2\pi r)^{-1/2}Re\{[1/(\mu_1-\mu_2)][\mu_2^2(\cos\theta+\mu_2\sin\theta)^{-1/2}-\mu_1^2(\cos\theta+\mu_1\sin\theta)^{-1/2}]\}+K_{II}(\pi a)^{-1/2}Re\{\mu_1+\mu_2\}+0[(r/a)^{1/2}]$$

$$\sigma_y = K_{II}(2\pi r)^{-1/2}Re\{[1/(\mu_1-\mu_2)][(\cos\theta+\mu_2\sin\theta)^{-1/2}-(\cos\theta+\mu_1\sin\theta)^{-1/2}]\}+0[(r/a)^{1/2}] \quad (5)$$

$$\tau_{xy} = K_{II}(2\pi r)^{-1/2}Re\{[1/(\mu_1-\mu_2)][\mu_1(\cos\theta+\mu_1\sin\theta)^{-1/2}-\mu_2(\cos\theta+\mu_2\sin\theta)^{-1/2}]\}+0[(r/a)^{1/2}]$$

The results shown in Eqs. (3) and (5) are similar to those obtained for the isotropic case in that for sufficiently small values of r/a, the series may be truncated to their first terms without significantly altering their accuracy. Thus, the stress field within the crack-tip region is characterized by a stress intensity factor in both isotropic and anisotropic materials; moreover, since the material anisotropy is completely characterized by μ_1 and μ_2, the stress intensity factor is the same function of loading conditions and geometry in both isotropic and anisotropic materials. The extension of standard LEFM procedures to advanced fiber composite materials should therefore permit the direct application of the many stress intensity factors already calculated, as functions of loading mode and structural geometry, for finite specimens of isotropic materials.[5,6] However, this prediction is based on the assumed validity of a homogeneous continuum material model for fiber composite materials; utilization of the analytical model discussed above is therefore dependent on the verification of this assumption.

Experimental Data

Test Program and Data Reduction

In order to verify the assumption that a heterogeneous fiber composite material may be modelled as a homogeneous continuum, a pilot series of experiments, patterned after valid fracture tests in metals,[6] was performed.[7] Twenty-three edge-notched specimens of various laminates of a graphite/epoxy material system, having initial notches of various lengths, were broken in three-point bending (Fig. 2). A value of K_Q, the stress intensity factor corresponding to incipient crack growth, was obtained from the test data for each of the specimens tested, using a relationship of the form

$$K_Q = P_Q(a)^{1/2}F \quad (6)$$

where P_Q is the experimentally determined load corresponding to crack extension in the specimen, a is the crack length, and F is a known function of specimen geometry.[6]

It should be noted that the formal validity of these tests could not be established, there being no criteria for a valid fracture test in an advanced fiber composite material; thus, the value of the stress intensity factor characterizing crack growth in a composite laminate may not be designated a critical stress intensity factor K_{IC}. Nevertheless, the values of K_Q, the candidate stress intensity factor obtained from the test series, though not formally valid, are apparent material properties of the various laminates tested. Since a material parameter does seem to characterize crack growth in the laminates tested, as predicted by the analytical model, a homogeneous model of these particular fiber composite materials does appear to be valid.

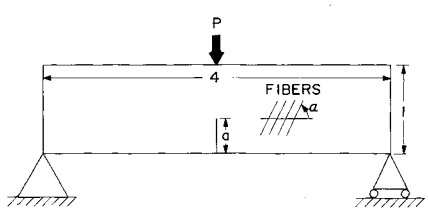

Fig. 2 Three-point bend specimen. Crack-length denoted by a, fiber direction by α. All dimensions in inches.

Analysis of Experimental Data

Although K_Q does characterize crack growth in a given composite laminate subjected to given loading conditions, it is not a completely satisfactory parameter for comparisons among different laminates. This is attributable to the possible presence of tension-shear coupling in composite materials, which can induce both Mode I and Mode II behavior at the crack-tip in response to either Mode I or Mode II loading. In such a situation, it is clear from (6) that, although K_Q will reflect the presence of both modes of crack-tip behavior, the coupling between these modes will not be explicitly known. Although, as is discussed below, K_Q may be decomposed into Mode I and Mode II components (K_{IQ} and K_{IIQ}, respectively) the problem of comparing different laminates remains, since two material parameters are now involved.

A more satisfactory characterization of crack behavior is obtained from $\mathcal{G}_Q$, the strain energy release rate corresponding to collinear crack growth in a composite laminate.

The value of $\mathcal{G}_Q$ may be shown to be[3]

$$\mathcal{G}_Q = (K_{IIQ}^2\beta_{11}/2)Im\{\mu_1+\mu_2\}+(K_{IQ}K_{IIQ}/2)Im\{\beta_{11}\mu_1\mu_2-\beta_{22}/\mu_1\mu_2\}-(K_{IQ}^2\beta_{22}/2)Im\{(\mu_1+\mu_2)/\mu_1\mu_2\} \quad (7)$$

It is obvious from (7) that $\mathcal{G}_Q$ may be easily calculated for any laminate, once K_Q has been decomposed into K_{IQ} and K_{IIQ}.

The Mode I and Mode II components of K_Q may be decoupled by combining the stress analysis results given by Eqs. (3) and (5) with a numerical calculation of the stress field in the crack-tip region. The stress analysis results corresponding to mixed mode behavior at the crack-tip are found by superposing Eqs. (3) and (5). Evaluating this combined stress field on the crack-axis ($\theta = 0°$, Fig. 1) yields

$$\sigma_x = (2\pi r)^{-1/2}[K_I Re\{-\mu_1\mu_2\}+K_{II}Re\{-\mu_1-\mu_2\}]$$
$$\sigma_y = K_I(2\pi r)^{-1/2} \quad (8)$$
$$\tau_{xy} = K_{II}(2\pi r)^{-1/2}$$

for sufficiently small values of r. Taking the logarithm of the last two expressions of Eq. (8) yields

$$\ln\sigma_y = \ln[K_I(2\pi)^{-1/2}]-\tfrac{1}{2}\ln[r]$$
$$\ln\tau_{xy} = \ln[K_{II}(2\pi)^{-1/2}]-\tfrac{1}{2}\ln[r] \quad (9)$$

To obtain K_I and K_{II} from (9), it is necessary to know σ_y and τ_{xy} as functions of r along the crack-axis. For this purpose, a finite element analogue of the laboratory experiments was employed. The three-point bend specimen geometry used in the experimental work was modelled by a two-dimensional grid of linear displacement triangular elements; the composite laminates tested in the experimental program were modelled as homogeneous continua, using lamination theory.[2] The model of the experimental specimen thus obtained was then analyzed when subjected to three-point bending by a load P_Q, the experimentally determined load corresponding to crack growth in the specimen being considered. Therefore, the finite element results describe the

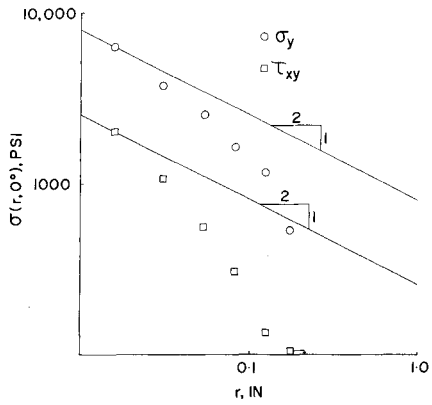

Fig. 3 Finite element data for the stress field on the crack-axis vs distance from the crack-tip.

state of the experimental specimen at the condition of incipient crack growth. The solution of this 714 degree-of-freedom problem required approximately two minutes of UNIVAC 1108 time.

From the finite element analysis, values of σ_y and τ_{xy} are obtained at a number of locations on the crack-axis. These stress values are plotted, on a logarithmic scale, against $\ln r$ (Fig. 3). Straight lines of slope $-\frac{1}{2}$ are then fitted to these data within the crack-tip region. These lines are the graphical representation of the equations given in Eq. (9), and thus determine values of K_I and K_{II}. Moreover, since these lines are based on finite element data which represent the experimental specimens at the condition of incipient crack growth, the values obtained for K_I and K_{II} are actually K_{IQ} and K_{IIQ}, the Mode I and Mode II components of K_Q. With these values known, the calculation of $\mathcal{G}_Q$ becomes a simple algebraic exercise.

An equally valid, and much less complex method of obtaining a value of the strain energy release rate characteristic of collinear crack growth in a composite laminate is to evaluate J, Rice's J-integral[8]

$$J = \int_\Gamma \{W\,dy - [\mathbf{T}\cdot\partial\mathbf{u}/\partial x]\,ds\} \qquad (10)$$

where Γ is a curve surrounding the crack-tip, W is the strain energy, (x,y) are coordinate directions, $\mathbf{T}$ is the traction vector on Γ, $\mathbf{u}$ is the displacement vector on Γ, and ds is an element of Γ (Fig. 4). If Eq. (10) is evaluated at the condition of incipient crack growth, the result J_Q is exactly equivalent to $\mathcal{G}_Q$ for linear elastic materials. Thus, by calculating J in the finite element analysis (which models the specimen at the condition of incipient crack growth) the value of J_Q (or $\mathcal{G}_Q$) is directly obtained. The method suggested by Hayes[9] was used to calculate J_Q within the finite element program.

It should be noted that Eq. (7) is a valid expression only in those cases in which the path of crack growth is at least initially collinear with the existing crack. Moreover, J_Q is equivalent to $\mathcal{G}_Q$ only if this same collinearity of crack path

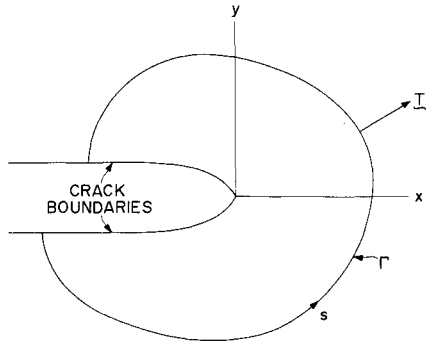

Fig. 4 Coordinate system and integration path for Rice's J-integral.[8]

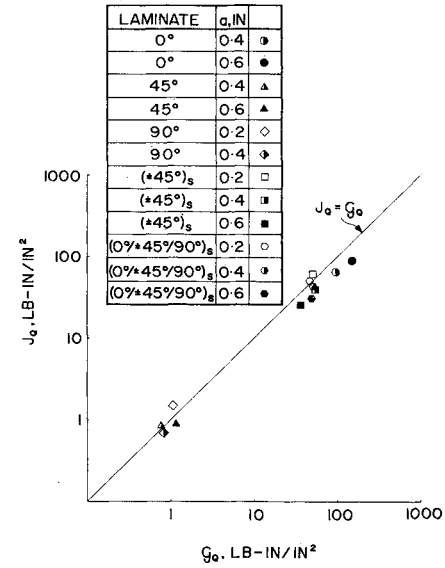

Fig. 5 J_Q vs $\mathcal{G}_Q$. Note the segregation of the data into two distinct groups.

and initial crack exists. Thus, for some of the specimens tested, in which the path of initial crack extension was not collinear with the original crack,[7] the calculation of $\mathcal{G}_Q$ and J_Q according to Eqs. (7) and (10) is not strictly correct. Such calculations were nevertheless performed for these specimens, simply because no viable alternative means of correctly evaluating the desired strain energy release rates were available.

Results and Conclusions

The values obtained for J_Q and $\mathcal{G}_Q$ are shown, in cross-plotted form, in Fig. 5. As can be seen, the data points are segregated into two distinct groups, separated by approximately two orders of magnitude. The high energy group consists of those laminates in which the experimentally observed fracture path crossed, i.e., broke, fibers. This group of specimens is discussed elsewhere.[10] The low energy group consists of those laminates in which the experimentally observed path of crack growth lay between fibers.

This low energy group of laminates is especially interesting because of the significant differences in experimental behavior exhibited by these laminates. In the laminate $\alpha = 45°$, both Mode I and Mode II behavior are present at the crack-tip, and the path of crack growth is not collinear with the original crack; in the laminate $\alpha = 90°$, only Mode I behavior is present at the crack-tip, and the path of crack growth is collinear with

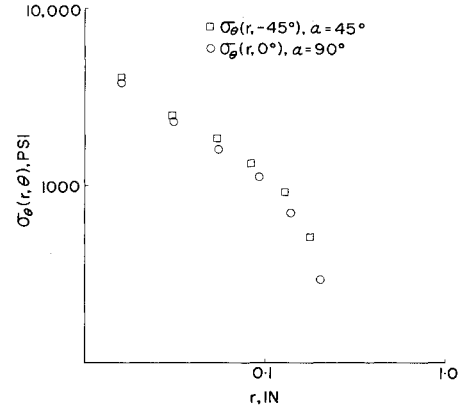

Fig. 6 Hoop stress on the fracture path in laminates of the low-energy group.

the original crack. That a single value of the strain energy release rate should characterize two so apparently unlike types of behavior seems rather curious.

This anomaly may be resolved by considering the common factor between the laminates of the low energy group, viz., in each of these laminates, crack growth occurred by matrix failure. Thus, the $\mathcal{G}_Q$ values obtained for these laminates actually characterize the in situ fracture toughness of only the matrix material. Since the matrix material is the same in both laminates, it follows that the $\mathcal{G}_Q$ values for both laminates should be the same, as they are.

A further characterization of matrix fracture is obtained by comparing the stress component normal to the experimentally determined fracture path (i.e., the hoop stress on the fracture path) in the laminates of the low energy group at the conditions at which crack growth initiated. Such a comparison is shown in Fig. 6, using finite element data. Clearly, the crack extends into the same tensile stress field in both laminates of the low energy group, even though the paths and modes of crack growth are very different in each of the two laminates. It is thus suggested that matrix fracture is stress-governed, regardless of the mode or direction of crack growth.

References

[1] Williams, M. L., "On the Stress Distribution at the Base of a Stationary Crack," *Journal of Applied Mechanics*, Vol. 24, No. 1, March 1957, pp. 109–114.

[2] Ashton, J. E., Halpin, J. C., and Petit, P. H., *Primer on Composite Materials: Analysis*, 1st ed., Technomic Publishing, Stamford, Conn., 1969, pp. 6–92.

[3] Sih, G. C., Paris, P. C., and Irwin, G. R., "On Cracks in Rectilinearly Anisotropic Bodies," *International Journal of Fracture Mechanics*, Vol. 1, No. 3, Sept. 1965, pp. 189–203.

[4] Konish, H. J., Jr., "Stress Analysis of the Crack-Tip Region in a Cracked Anisotropic Plate," SM-64, June 1971, Dept. of Mechanical Engineering, Carnegie Inst. of Technology, Carnegie-Mellon Univ., Pittsburgh, Pa.

[5] Paris, P. C. and Sih, G. C., "Stress Analysis of Cracks," *Fracture Toughness Testing and its Applications, ASTM STP 381*, 1st ed., Vol. 1, American Society for Testing and Materials, Philadelphia, Pa., 1964, pp. 30–83.

[6] Srawley, J. E. and Brown, W. F., Jr., *Plane Strain Crack Toughness Testing in High Strength Metallic Materials, ASTM STP 410*, 1st ed., Vol. 1, American Society for Testing and Materials, Philadelphia, Pa., 1967.

[7] Konish, H. J., Jr., Swedlow, J. L., and Cruse, T. A., "Experimental Investigation of Fracture in an Advanced Fiber Composite," *Journal of Composite Materials*, Vol. 6, No. 1, Jan. 1972, pp. 114–124.

[8] Rice, J. R., "A Path Independent Integral and the Approximate Analysis of Strain Concentrations by Notches and Cracks," *Journal of Applied Mechanics*, Vol. 35, No. 2, June 1968, pp. 379–386.

[9] Hayes, D. J., "Some Applications of Elasto-Plastic Analysis to Fracture Mechanics," Doctoral dissertation, Oct. 1970, Dept. of Mechanical Engineering, Imperial College of Science and Technology, Univ. of London, London, England.

[10] Konish, H. J., Jr., Cruse, T. A., and Swedlow, J. L., "A Method for Estimating Fracture Strength of Specially Orthotropic Composite Laminates," SM-72-9, March 1972, Dept. of Mechanical Engineering, Carnegie Inst. of Technology, Carnegie-Mellon Univ., Pittsburgh, Pa.

JANUARY 1973 AIAA JOURNAL VOL. 11, NO. 1

A Force Field Theory: Part I. Laminar Flow Instability

JOSHUA C. ANYIWO*
Colorado State University, Fort Collins, Colo.

A force field theory is stated, namely, that: "The dynamic characteristics of a body in motion are completely determined by the forces (external and internal) acting on the body, either instantaneously or over a period in time or space." This theory facilitates the definition of a generalized Stability Number in terms of the Engineering Numbers that characteristically describe flows. It is shown that, as defined in this paper, the Stability Number and the position parameter are the necessary and sufficient parameters for describing the dynamic characteristics of flows, in general. Any flow becomes unstable to applied disturbances if the local Stability Number is greater than $N\phi(I_e)$, where N is a numerical constant and $\phi(I_e)$ is a function of the wall and freestream disturbance intensity. The value of N depends on whether the boundaries of the flow are rigid-rigid, rigid-free or free-free. $N = 10^3$ for rigid-free boundaries. The great simplicity and accuracy of this method makes it by far the most practicable for estimating flow instability.

Nomenclature

$A, B, \ldots Z$; $a, b, \ldots z$ = numerical constants
Ax; Ay = Transpiration number, $(U_1\Delta/\nu)(\nu_0/U_1)$; $(\nu_0\Delta/\nu)^2$
C = Wall curvature parameter, Δ/r_0
F = forcefield
G = Görtler number, $Re_\theta(\theta/r_0)^{1/2}$
H = Velocity Profile Shape Factor, δ^*/θ
I = local total disturbance intensity
i, j, k = indices
Mini (.) = minimum value of (.)
Pr = Prandtl number
r_0 = wall radius of curvature
Ra = Rayleigh number
Re = Reynolds number
Sn = section stability number
Ta = Taylor number
U_1 = freestream velocity
u = local streamwise velocity

Received March 20, 1972; revision received September 7, 1972. Research supported by NSF Grant GK-23989 from the Engineering Mechanics Division of the National Science Foundation is gratefully acknowledged.

Index category: Boundary-Layer Stability and Transition.

* Research Scientist. Associate Member AIAA.